

Article

# Fabrication and Magneto-Optical Property of $(\text{Dy}_{0.7}\text{Y}_{0.25}\text{La}_{0.05})_2\text{O}_3$ Transparent Ceramics by PLSH Technology

Ding Zhou <sup>1,\*</sup>, Xiaohui Li <sup>1</sup>, Tun Wang <sup>2</sup>, Jiayue Xu <sup>1</sup>, Zhanyong Wang <sup>1</sup>, Ying Shi <sup>2</sup>, Dmitry Permin <sup>3</sup> and Stanislav S. Balabanov <sup>3,\*</sup>

<sup>1</sup> School of Materials Science and Engineering, Shanghai Institute of Technology, Shanghai 201418, China; 196081105@mail.sit.edu.cn (X.L.); xujiayue@sit.edu.cn (J.X.); wzy2195@sit.edu.cn (Z.W.)

<sup>2</sup> School of Material Science and Engineering, Shanghai University, Shanghai 200444, China; wangtun@shu.edu.cn (T.W.); yshi@shu.edu.cn (Y.S.)

<sup>3</sup> G.G. Devyatkh Institute of Chemistry of High-Purity Substances of the Russian Academy of Sciences, 49 Tropinin Str., 603137 Nizhny Novgorod, Russia; permin@ihps-nnov.ru

\* Correspondence: dzhou@sit.edu.cn (D.Z.); balabanov@ihps-nnov.ru (S.S.B.)

Received: 16 November 2020; Accepted: 10 December 2020; Published: 15 December 2020



**Abstract:**  $(\text{Dy}_{0.7}\text{Y}_{0.25}\text{La}_{0.05})_2\text{O}_3$  magneto-optical transparent ceramics were successfully fabricated by pressureless sintering in reductive  $\text{H}_2$  atmosphere (PLSH). The raw powder of  $(\text{Dy}_{0.7}\text{Y}_{0.25}\text{La}_{0.05})_2\text{O}_3$  was synthesized by a modified self-propagating high-temperature synthesis (SHS) and sintered to transparent ceramics at 1400–1600 °C in a flowing  $\text{H}_2$  atmosphere, showing good sinterability of the as-synthesized raw powder. The magneto-optical Verdet constant of  $(\text{Dy}_{0.7}\text{Y}_{0.25}\text{La}_{0.05})_2\text{O}_3$  transparent ceramics was measured to be  $-191.57 \text{ rad}/(\text{T}\cdot\text{m})$  at a wavelength of 632.8 nm. In this magneto-optical material of  $(\text{Dy}_{0.7}\text{Y}_{0.25}\text{La}_{0.05})_2\text{O}_3$ , relative cheaper Dy and Y were used to replace Tb, and the low cost and good magneto-optical property showed the advantage of application on Faraday isolators (FIs) and Faraday rotators (FRs).

**Keywords:**  $(\text{Dy}_{0.7}\text{Y}_{0.25}\text{La}_{0.05})_2\text{O}_3$ ; transparent ceramics; magneto-optical property; rare earth sesquioxide

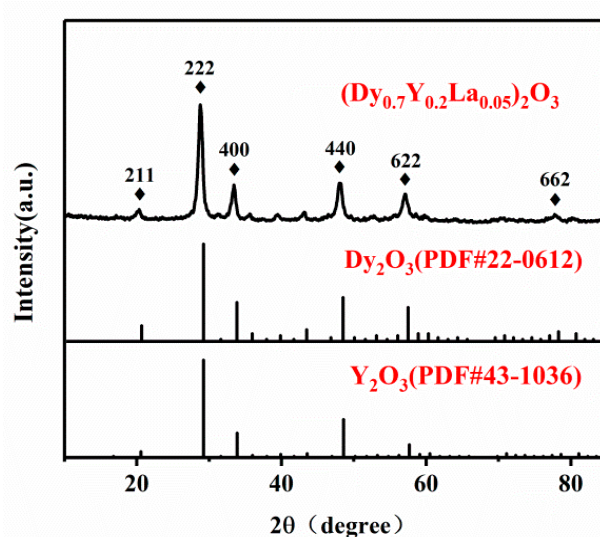
## 1. Introduction

Magneto-optical (M-O) material is an essential component of Faraday isolators (FIs) and Faraday rotators (FRs), which can be used in fiber-optic communication to effectively isolate external light from the light sources [1–3]. With the development of science and technology, FI and FR devices are also developing towards miniaturization, which puts forward higher requirement on the performance of M-O materials.  $\text{Tb}_3\text{Ga}_5\text{O}_{12}$  (TGG) with garnet structure is widely used as a magneto-optical material, and its Verdet constant is  $-134 \text{ rad}/(\text{T}\cdot\text{m})$  [4] at 632.8 nm. However, the garnet structure limits the terbium concentration of  $\text{Tb}^{3+}$  and therefore limits the Verdet constant [5]. In recent years, it has been found that rare-earth sesquioxide  $\text{RE}_2\text{O}_3$  ( $\text{RE} = \text{Tb}, \text{Dy}$ ) of paramagnetic  $\text{RE}^{3+}$  ions has a higher Verdet constant than TGG crystal [6–8]. In 2015, Veber et al. [6] grew the firstly  $\text{Tb}_2\text{O}_3$  single crystal with a size of about  $5 \times 5 \times 2 \text{ mm}^3$  by flux method. The Verdet constant of single crystal  $\text{Tb}_2\text{O}_3$  is at least three times larger than that of a commercial TGG crystal. In 2018, Snetkov and Balabanov et al. [9] prepared Y, La-doped  $(\text{Dy}_x\text{Y}_{0.95-x}\text{La}_{0.05})_2\text{O}_3$  transparent ceramics using a vacuum sintering method at an extremely high temperature of 1780 °C. Recently, Aung et al. [10] showed the possibility of obtaining ceramics  $(\text{Dy}_{0.7}\text{Y}_{0.25}\text{La}_{0.05})_2\text{O}_3$  with  $\text{ZrO}_2$  sintering aid. Despite the high achieved quality of ceramics, the use of such a sintering additive can limit the service life of magneto-optical elements due to a change in the oxidation state of zirconium ions under the laser radiation, the appearance of free charge carriers and, accordingly, a sharp increase in absorption.

In this paper, 5 at. % lanthanum oxide was used as sintering aid.  $(\text{Dy}_{0.7}\text{Y}_{0.25}\text{La}_{0.05})_2\text{O}_3$  powders were synthesized by self-propagating high-temperature synthesis (SHS) method. The transparent ceramics of  $(\text{Dy}_{0.7}\text{Y}_{0.25}\text{La}_{0.05})_2\text{O}_3$  was obtained by pressureless sintering in reductive  $\text{H}_2$  atmosphere (PLSH) technology at relatively low temperature. The microstructure, optical quality and magneto-optical Verdet constant of the ceramics were characterized as well.

## 2. Results and Discussion

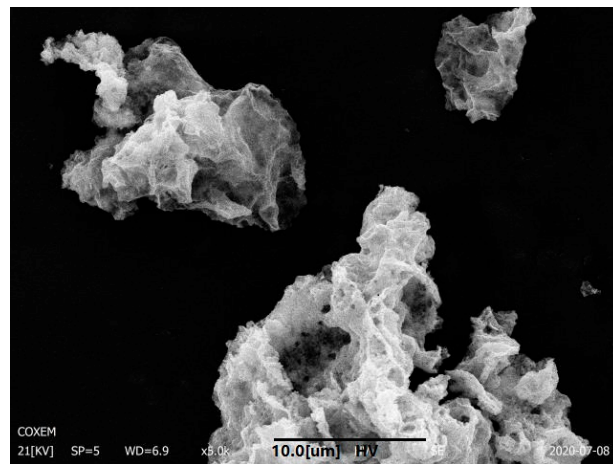
Figure 1 shows the X-ray diffraction pattern of  $(\text{Dy}_{0.7}\text{Y}_{0.25}\text{La}_{0.05})_2\text{O}_3$  powder synthesized by SHS method. It can be seen from the figure that the diffraction peaks of the  $(\text{Dy}_{0.7}\text{Y}_{0.25}\text{La}_{0.05})_2\text{O}_3$  powder corresponds to the  $\text{Dy}_2\text{O}_3$  and  $\text{Y}_2\text{O}_3$  standard cards (PDF#22-0612, PDF#43-1036). The main diffraction peaks of the powder are located between the peaks of two standard cards, indicating that  $\text{Y}_2\text{O}_3$  have entered the crystal lattice of  $\text{Dy}_2\text{O}_3$  and they formed a substitutional solid solution. The crystal grain size of  $(\text{Dy}_{0.7}\text{Y}_{0.25}\text{La}_{0.05})_2\text{O}_3$  powder is 15.5 nm, calculated by the Scherrer formula.



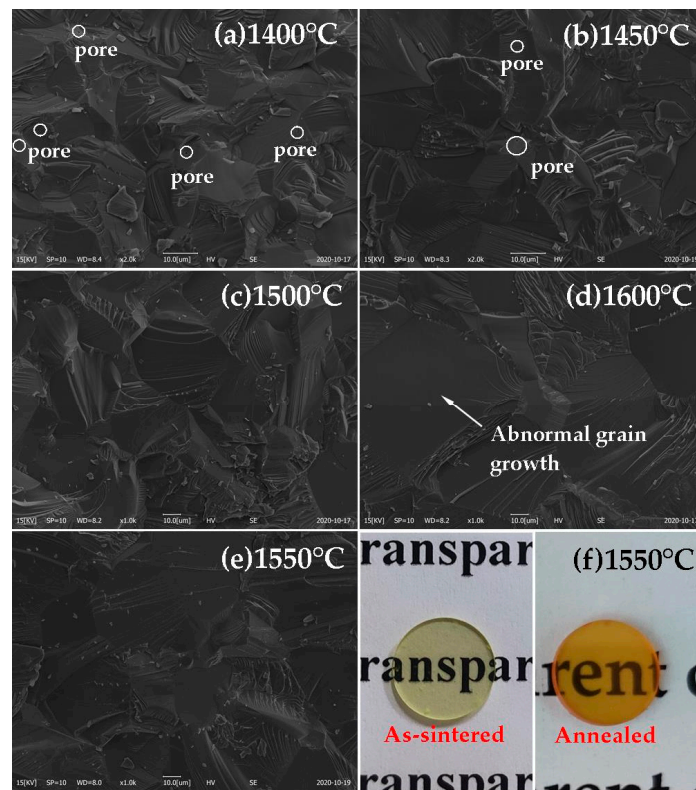
**Figure 1.** X-ray diffraction pattern of  $(\text{Dy}_{0.7}\text{Y}_{0.25}\text{La}_{0.05})_2\text{O}_3$  powder.

Figure 2 is a scanning electron microscope image of  $(\text{Dy}_{0.7}\text{Y}_{0.25}\text{La}_{0.05})_2\text{O}_3$  powder synthesized by SHS. The powders consist of irregular primary particles, which are combined to form loose agglomerates with a porous structure [11]. The formation of this structure is determined by the mechanism of the SHS, where the propagation of the reaction front causes the precursor to foam, followed by the start of the combustion reaction and the discharge of a large amount of gaseous product [12–14].

To characterize the microstructure of as-sintered transparent ceramics, the fracture of  $(\text{Dy}_{0.7}\text{Y}_{0.25}\text{La}_{0.05})_2\text{O}_3$  ceramic is observed by SEM. As shown in the Figure 3a, there are many micro-pores in the ceramics sintered at 1400 °C by PLSH technology. When the temperature increased to 1450 °C, a small amount of pores can still be found in the ceramic matrix, marked with white circles, as shown in Figure 3b. It is demonstrated in Figure 3c,e that the ceramics have homogeneous microstructures without abnormal grain growth and the fracture mode of  $(\text{Dy}_{0.7}\text{Y}_{0.25}\text{La}_{0.05})_2\text{O}_3$  transparent ceramics is mainly trans-granular. However, in Figure 3d, abnormal grain growth can be observed in 1600 °C PLSH sintered ceramic, which leads to the degradation of optical transmittance in the visible wavelength to a certain extent. The appearance of the  $(\text{Dy}_{0.7}\text{Y}_{0.25}\text{La}_{0.05})_2\text{O}_3$  transparent ceramics, before and after annealing at 900 °C for 5 h in air are shown in the Figure 3f. The transmittance curves of  $(\text{Dy}_{0.7}\text{Y}_{0.25}\text{La}_{0.05})_2\text{O}_3$  transparent ceramics before and after annealing at 900 °C in a muffle furnace are given in Figure 4. Annealing in air did not affect the transmittance in the infrared range of the spectrum, but reduced the transmission in the visible range.



**Figure 2.** Scanning electron microscope micrograph of  $(\text{Dy}_{0.7}\text{Y}_{0.25}\text{La}_{0.05})_2\text{O}_3$  powder prepared by self-propagating high-temperature synthesis (SHS).



**Figure 3.** SEM micrographs of the fracture surface of  $(\text{Dy}_{0.7}\text{Y}_{0.25}\text{La}_{0.05})_2\text{O}_3$  ceramics: (a) 1400 °C/6 h; (b) 1450 °C/6 h; (c) 1500 °C/6 h; (d) 1600 °C/6 h; (e) 1550 °C/6 h; (f) the appearance of the  $(\text{Dy}_{0.7}\text{Y}_{0.25}\text{La}_{0.05})_2\text{O}_3$  transparent ceramics sintered at 1550 °C: as-sintered and annealed at 900 °C for 5 h in air.

The transmittance in the IR range (1895 nm to 2000 nm) is significantly higher than that previously published on ceramics of the same composition [9] and in  $\text{Dy}_2\text{O}_3$  transparent ceramics with  $\text{ZrO}_2$  sintering aid by vacuum sintering [10]. Therefore, PLSH sintering should be recognized as an effective method for producing transparent ceramics. However, the existing scattering in the visible range in such ceramics indicates the presence of defects on the nanoscale-submicron scale. There is a possibility that with a large element length required for an FI (about 25 mm at a magnetic field of 2.5 T), scattering by these defects can become noticeable at a wavelength of 2000 nm. The Verdet constant of

$(\text{Dy}_{0.7}\text{Y}_{0.25}\text{La}_{0.05})_2\text{O}_3$  transparent ceramics is  $-191.57 \text{ rad}/(\text{T}\cdot\text{m})$  ( $\lambda = 632.8 \text{ nm}$ ), which is 1.43 times that of a commercial TGG crystal.

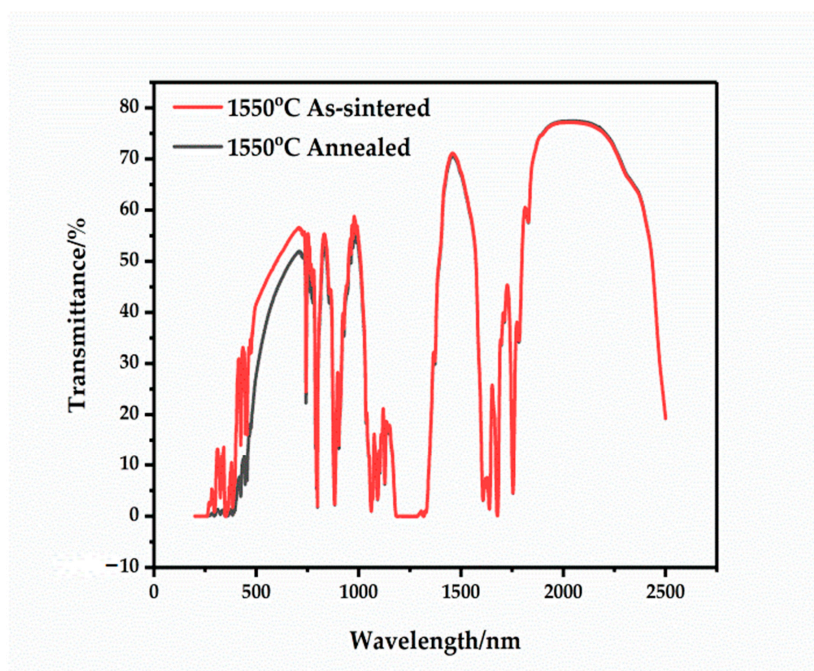


**Figure 4.** Transmittance curves of the  $(\text{Dy}_{0.7}\text{Y}_{0.25}\text{La}_{0.05})_2\text{O}_3$  ceramics: as-sintered and additionally annealed at  $900 \text{ }^\circ\text{C}$  for 5 h in air.

Figure 5 shows X-ray diffraction patterns of  $(\text{Dy}_{0.7}\text{Y}_{0.25}\text{La}_{0.05})_2\text{O}_3$  ceramics before and after annealing at  $900 \text{ }^\circ\text{C}$  for 5 h in air. After annealing in air, the XRD data completely coincide with the card (PDF#22-0612) for cubic  $\text{Dy}_2\text{O}_3$ ; the relative intensities of the peaks also correspond to these data, and no impurities or secondary phases are detected. In the as-sintered  $(\text{Dy}_{0.7}\text{Y}_{0.25}\text{La}_{0.05})_2\text{O}_3$  ceramic, the relative intensities of the peaks significantly deviate from the card (PDF#22-0612) for cubic  $\text{Dy}_2\text{O}_3$ . However, the peak at  $2\theta = 26^\circ$  is not related to  $\text{Dy}_2\text{O}_3$  but coincides with the  $\text{La}_2\text{O}_3$  (PDF#05-0602). It can be associated with a significant effect of oxygen vacancies and, probably,  $\text{Dy}^{2+}$  ions on the phase formation in the  $\text{Dy}_2\text{O}_3$ - $\text{Y}_2\text{O}_3$ - $\text{La}_2\text{O}_3$  system. When the ceramic sample is annealed in the muffle furnace at  $900 \text{ }^\circ\text{C}$  for 5 h, the  $\text{La}_2\text{O}_3$  phase disappeared, characterized by XRD, as shown in Figure 5. After annealing, the  $\text{Dy}^{2+}$  ions are oxidized, oxygen vacancies decrease, and the solubility of  $\text{La}_2\text{O}_3$  in the solid solution increases. We attribute the decrease in the transmission of ceramics in the visible range after annealing in air to the presence of hydrogen in residual pores and interstices.

Further progress in improving the quality of ceramics  $(\text{Dy}_{0.7}\text{Y}_{0.25}\text{La}_{0.05})_2\text{O}_3$  can be associated with a thorough study of the phase diagrams in this system, taking into account the calcination atmosphere and finding the exact technological path to prevent the formation of secondary phases. Another or parallel possibility is to change the sintering technological route. Moreover, the combination of PLSH sintering at a low temperature (about  $1400 \text{ }^\circ\text{C}$ ) with subsequent hot isostatic pressing (HIP) and annealing in air seems to be promising.

The magneto-optical Verdet constant, which was recorded by the magneto-optical measurement system with a He-Ne laser, two polarizers and an electromagnet coil, was measured to be  $-191.57 \text{ rad}/(\text{T}\cdot\text{m})$  at a wavelength of  $632.8 \text{ nm}$ , which is 1.43 times larger than that of commercial terbium gallium garnet ( $\text{Tb}_3\text{Ga}_5\text{O}_{12}$ , TGG) crystal. Andrzej Kruk et al. [15] proposed using MO-FOM (magneto-optical figure of merit) factor to describe the comprehensive magneto-optical property of Faraday materials. In this paper, the FOM of the  $(\text{Dy}_{0.7}\text{Y}_{0.25}\text{La}_{0.05})_2\text{O}_3$  transparent ceramic is calculated to be  $0.66584 \text{ rad}/\text{T}$  ( $38.15\text{deg}/\text{T}$ ), which shows good prospects for magneto-optical applications.

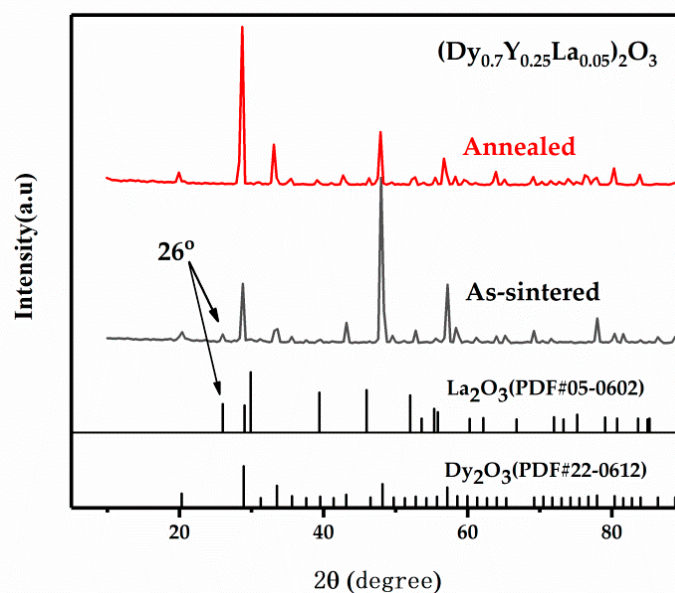


Figure 5. XRD pattern of  $(\text{Dy}_{0.7}\text{Y}_{0.25}\text{La}_{0.05})_2\text{O}_3$  ceramic before and after annealing at 900 °C for 5 h in air.

### 3. Materials and Methods

The powder of  $(\text{Dy}_{0.7}\text{Y}_{0.25}\text{La}_{0.05})_2\text{O}_3$  was synthesized by a technique of self-propagating high-temperature synthesis (SHS) method, which was described in detail in previous research [16–19]. The raw material of the powder of  $(\text{Dy}_{0.7}\text{Y}_{0.25}\text{La}_{0.05})_2\text{O}_3$  was dysprosium oxide 99.99% (Polirit, Moscow, Russia), yttrium oxide 99.99% (Polirit, Moscow, Russia), lanthanum oxide 99.99% (Polirit, Moscow, Russia), nitric acid 99.9999% (Khimreaktiv, Nizhny Novgorod, Russia), glycine  $\text{NH}_2\text{CH}_2\text{COOH}$  99.9% (Khimreaktiv, Nizhny Novgorod, Russia). The stoichiometric amount of metal cations dysprosium, yttrium and lanthanum are prepared by dissolving the respective metal oxides in nitric acid mixed water under heating. The concentration of the solution was determined by the gravimetric method at 1100 °C. Then, the nitrate solution is diluted to the desired concentration. Moreover, the solution of glycine and the metal nitrates was prepared with the ratio of 1:1. The SHS redox reactions of precursor in a quartz flask were initiated in the furnace preheated at 500 °C. Then, the highly dispersed powders were formed. The  $(\text{Dy}_{0.7}\text{Y}_{0.25}\text{La}_{0.05})_2\text{O}_3$  powder was pressed and sintered in a flowing hydrogen atmosphere at 1400–1600 °C for 6 h to obtain  $(\text{Dy}_{0.7}\text{Y}_{0.25}\text{La}_{0.05})_2\text{O}_3$  ceramics.

The X-ray diffractometer (Rigaku, Tokyo, Japan) as the detective method equipped with graphite monochromatized Cu  $K\alpha$  radiation ( $\lambda = 1.5406 \text{ \AA}$ , 40 kV/200 mA) was used to investigate the crystal structure of ceramic powders in the range of  $2\theta = 10\text{--}80^\circ$ . The microscopic morphology of the samples was determined by the scanning electron microscope (COXEM, Daejeon, Korea). The UV-vis-NIR spectrophotometer (Agilent, Palo Alto, CA, USA) was used to record the linear transmittance of transparent ceramics. The device of the magneto-optical measurement system (Fudan Tianxin, Shanghai, China) was used to measure the Verdet constant at 632.8 nm. The crystal grain size of  $(\text{Dy}_{0.7}\text{Y}_{0.25}\text{La}_{0.05})_2\text{O}_3$  powder calculated by Sherer formula [20]:

$$D = K\lambda/B\cos\theta \quad (1)$$

### 4. Conclusions

$(\text{Dy}_{0.7}\text{Y}_{0.25}\text{La}_{0.05})_2\text{O}_3$  powder was synthesized by the self-propagating high-temperature synthesis method. The compact green bodies of  $(\text{Dy}_{0.7}\text{Y}_{0.25}\text{La}_{0.05})_2\text{O}_3$  can be sintered to be transparent ceramics by pressureless sintering in a reductive  $\text{H}_2$  atmosphere method at 1400–1600 °C. The inline transmittance of 1550 °C sintered ceramic at 2000 nm was measured to be 78%, which is the highest published

inline transmittance till now. Further improvement of the optical quality in the visible range of  $(\text{Dy}_{0.7}\text{Y}_{0.25}\text{La}_{0.05})_2\text{O}_3$  ceramics shed light on the application of magneto-optical isolators.

**Author Contributions:** Conceptualization, D.Z. and S.S.B.; methodology, J.X., Z.W. and Y.S.; software, X.L. and T.W.; writing—original draft preparation, X.L.; writing—review and editing, D.Z., S.S.B. and D.P. All authors have read and agreed to the published version of the manuscript.

**Funding:** This research was funded by National Science Foundation of China, grant number U1732128 and partially by the Research Project of the Russian Science Foundation (No. 18-13-00355).

**Conflicts of Interest:** The authors declare no conflict of interest.

## References

1. Dai, J.W.; Li, J. Promising magneto-optical ceramics for high power Faraday isolators. *Scr. Mater.* **2018**, *155*, 78–84. [[CrossRef](#)]
2. Yang, M.; Zhou, D.; Xu, J.; Tian, T.; Jia, R.; Wang, Z. Fabrication and magneto-optical property of yttria stabilized  $\text{Tb}_2\text{O}_3$  transparent ceramics. *J. Eur. Ceram. Soc.* **2019**, *39*, 5005–5009. [[CrossRef](#)]
3. Banerjee, S.; Ertel, K.; Mason, P.D.; Phillips, P.J.; Siebold, M.; Loeser, M.; Hernandez-Gomez, C.; Collier, J.L. High-efficiency 10 J diode pumped cryogenic gas cooled Yb:YAG multislabs amplifier. *Opt. Lett.* **2012**, *37*, 2175–2177. [[CrossRef](#)] [[PubMed](#)]
4. Kaminskii, A.A.; Eichler, H.J.; Reiche, P.; Uecker, R. SRS risk potential in Faraday rotator  $\text{Tb}_3\text{Ga}_5\text{O}_{12}$  crystals for high-peak power lasers. *Laser Phys. Lett.* **2005**, *2*, 489–492. [[CrossRef](#)]
5. Balabanov, S.S.; Permin, D.A.; Rostokina, E.Y.; Palashov, O.V.; Snetkov, I.L. Characterizations of REE:  $\text{Tb}_2\text{O}_3$  Magneto-Optical Ceramics. *Phys. Status Solidi B* **2020**, *257*, 1900474. [[CrossRef](#)]
6. Veber, P.; Velázquez, M.; Gadret, G.; Rytz, D.; Peltz, M.; Decourt, R. Flux growth at 1230 °C of cubic  $\text{Tb}_2\text{O}_3$  single crystals and characterization of their optical and magnetic properties. *CrystEngComm* **2015**, *17*, 492–497. [[CrossRef](#)]
7. Furuse, H.; Yasuhara, R. Magneto-optical characteristics of holmium oxide ( $\text{Ho}_2\text{O}_3$ ) ceramics. *Opt. Mater. Express* **2017**, *7*, 827–833. [[CrossRef](#)]
8. Morales, J.R.; Amos, N.; Khizroev, S.; Garay, J.E. Magneto-optical Faraday effect in nanocrystalline oxides. *J. Appl. Phys.* **2011**, *109*, 093110. [[CrossRef](#)]
9. Snetkov, I.L.; Yakovlev, A.I.; Permin, D.A.; Balabanov, S.S.; Palashov, O.V. Magneto-optical Faraday effect in dysprosium oxide ( $\text{Dy}_2\text{O}_3$ ) based ceramics obtained by vacuum sintering. *Opt. Lett.* **2018**, *43*, 4041–4044. [[CrossRef](#)] [[PubMed](#)]
10. Aung, Y.L.; Ikesue, A.; Yasuhara, R.; Iwamoto, Y. Magneto-optical  $\text{Dy}_2\text{O}_3$  ceramics with optical grade. *Opt. Lett.* **2020**, *45*, 4615–4617. [[CrossRef](#)] [[PubMed](#)]
11. Balabanov, S.; Filofeev, S.; Ivanov, M.; Kaigorodov, A.; Krugovykh, A.; Kuznetsov, D.; Permin, D.; Popov, P.; Rostokina, E. Fabrication and characterizations of erbium oxide based optical ceramics. *Opt. Mater.* **2020**, *101*, 109732. [[CrossRef](#)]
12. Permin, D.A.; Balabanov, S.S.; Novikova, A.V.; Snetkov, I.L.; Palashov, O.V.; Sorokin, A.A.; Ivanov, M.G. Fabrication of Yb-doped  $\text{Lu}_2\text{O}_3$ - $\text{Y}_2\text{O}_3$ - $\text{La}_2\text{O}_3$  solid solutions transparent ceramics by self-propagating high-temperature synthesis and vacuum sintering. *Ceram. Int.* **2019**, *45*, 522–529. [[CrossRef](#)]
13. Permin, D.A.; Boldin, M.S.; Belyaev, A.V.; Balabanov, S.S.; Novikova, A.V.; Koshkin, V.A.; Murashov, A.A.; Ladenkov, I.V.; Popov, A.A.; Lantsev, E.A.; et al. IR-transparent  $\text{MgO}$ - $\text{Y}_2\text{O}_3$  ceramics by self-propagating high-temperature synthesis and spark plasma sintering. *Ceram. Int.* **2020**, *46*, 15786–15792. [[CrossRef](#)]
14. Permin, D.A.; Balabanov, S.S.; Snetkov, I.L.; Palashov, O.V.; Novikova, A.V.; Klyusik, O.N.; Ladenkov, I.V. Hot pressing of Yb: $\text{Sc}_2\text{O}_3$  laser ceramics with LiF sintering aid. *Opt. Mater.* **2020**, *100*, 109701. [[CrossRef](#)]
15. Kruk, A.; Brylewski, T.; Mrózek, M. Optical and magneto-optical properties of  $\text{Nd}_{0.1}\text{La}_{0.1}\text{Y}_{1.8}\text{O}_3$  transparent ceramics. *J. Lumin.* **2019**, *209*, 333–339. [[CrossRef](#)]
16. Permin, D.A.; Novikova, A.V.; Gavrishchuk, E.M.; Balabanov, S.S.; Sorokin, A.A. Self-Propagating High-Temperature Synthesis of  $\text{Lu}_2\text{O}_3$  Powders for Optical Ceramics. *Inorg. Mater.* **2017**, *53*, 1330–1335. [[CrossRef](#)]
17. Permin, D.A.; Gavrishchuk, E.M.; Klyusik, O.N.; Novikova, A.V.; Sorokin, A.A. Preparation of optical ceramics based on highly dispersed powders of scandium oxide. *J. Opt. Technol.* **2018**, *85*, 58–62. [[CrossRef](#)]

18. Permin, D.A.; Kurashkin, S.V.; Novikova, A.V.; Savikin, A.P.; Gavrishchuk, E.M.; Balabanov, S.S.; Khamaletdinovaa, N.M. Synthesis and luminescence properties of Yb-doped  $Y_2O_3$ ,  $Sc_2O_3$  and  $Lu_2O_3$  solid solutions nanopowders. *Opt. Mater.* **2018**, *77*, 240–245. [[CrossRef](#)]
19. Balabanov, S.S.; Permin, D.A.; Rostokina, E.Y.; Egorov, S.V.; Sorokin, A.A.; Kuznetsov, D.D. Synthesis and structural characterization of ultrafine terbium oxide powders. *Ceram. Int.* **2017**, *43*, 16569–16574. [[CrossRef](#)]
20. Babayevskaya, N.V.; Deyneka, T.G.; Mateychenko, P.V.; Matveevskaya, N.A.; Tolmachev, A.V.; Yavetskiy, R.P. Fabrication and characterization of  $Lu_2O_3:Eu^{3+}$  nanopowders and X-ray films. *J. Alloys Compd.* **2010**, *507*, L26–L31. [[CrossRef](#)]

**Publisher's Note:** MDPI stays neutral with regard to jurisdictional claims in published maps and institutional affiliations.



© 2020 by the authors. Licensee MDPI, Basel, Switzerland. This article is an open access article distributed under the terms and conditions of the Creative Commons Attribution (CC BY) license (<http://creativecommons.org/licenses/by/4.0/>).